



Published in final edited form as:

*Biol Psychiatry*. 2015 September 15; 78(6): 361–373. doi:10.1016/j.biopsych.2014.12.012.

## Increased SNARE Protein-Protein Interactions in Orbitofrontal and Anterior Cingulate Cortices in Schizophrenia

Alfredo Ramos-Miguel, Clare L. Beasley, Andrew J. Dwork, J. John Mann, Gorazd Rosoklija, Alasdair M. Barr, and William G. Honer

BC Mental Health & Addictions Research Institute (AR-M, CLB, AMB, WGH), and Departments of Psychiatry (AR-M, CLB, WGH), and Pharmacology (AMB), University of British Columbia, Vancouver, BC, Canada; and Department of Psychiatry (AJD, JJM, GR), Columbia University, NY, USA

### Abstract

**Background**—Synaptic dysfunction in schizophrenia may be associated with abnormal expression or function of SNARE proteins (syntaxin, SNAP25, VAMP), forming the molecular complex underlying neurosecretion. The impact of such abnormalities on efficient SNARE heterotrimer formation is poorly understood. We investigated putative SNARE dysfunction, along with possible roles for the SNARE binding partners Munc18-1, complexins (Cplx) 1/2 and synaptotagmin, in brains from autopsies of individuals with and without schizophrenia.

**Methods**—Postmortem samples were obtained from orbitofrontal (OFC) and/or anterior cingulate (ACC) cortices from two separate cohorts ( $n = 15+15$  schizophrenia cases,  $n = 13+15$  controls). SNARE interactions were studied by immunoprecipitation and one- or two-dimensional blue native electrophoresis (BN-PAGE).

**Results**—In the first cohort, syntaxin, Munc18-1 and Cplx1, but not VAMP, Cplx2 or synaptotagmin, were two-fold enriched in SNAP25-immunoprecipitated products from schizophrenia OFC in the absence of any alterations in total tissue homogenate levels of these proteins. In BN-PAGE, the SNARE heterotrimer was identified as a 150-kDa complex, increased in schizophrenia samples from Cohort 1 (OFC: +45%; ACC: +44%) and Cohort 2 (OFC: +40%), with lower 70-kDa SNAP25-VAMP dimer (−37%) in the OFC. Upregulated 200-kDa SNARE-Cplx1 (+65%), and downregulated 550-kDa Cplx1-containing oligomers (−24%) in schizophrenia OFC were identified by BN-PAGE. These findings were not explained by postmortem interval, antipsychotic medication, or other potentially confounding variables.

---

Address correspondence to: Dr. W.G. Honer, Department of Psychiatry, University of British Columbia, 2255 Wesbrook Mall, Vancouver, BC, Canada, V6T 2A1. william.honer@ubc.ca.

**Publisher's Disclaimer:** This is a PDF file of an unedited manuscript that has been accepted for publication. As a service to our customers we are providing this early version of the manuscript. The manuscript will undergo copyediting, typesetting, and review of the resulting proof before it is published in its final citable form. Please note that during the production process errors may be discovered which could affect the content, and all legal disclaimers that apply to the journal pertain.

### Financial Disclosures

All other authors report no biomedical financial interests or potential conflicts of interest.

**Conclusions**—The findings support the hypothesis of upregulated SNARE complex formation in schizophrenia OFC, possibly favored by enhanced affinity for Munc18-1 and/or Cplx1. These alterations offer new therapeutic targets for schizophrenia.

### Keywords

schizophrenia; postmortem human brain; SNARE; complexin; Munc18-1; blue native PAGE

---

### Introduction

Schizophrenia is the major psychotic disorder, with an estimated lifetime prevalence range of .3-1% (1; 2). Compelling data support dopaminergic dysfunction as a source of psychosis-related symptoms, while glutamatergic hypofunction may also contribute to the schizophrenia syndrome (3-8). The clinical phenotypes are attributed to developmentally “miswired” neural connectivity between orbitofrontal cortex and hippocampus, as well as striatal and thalamic nuclei (8-12). A recent meta-analysis positron emission tomography studies in early schizophrenia found consistent abnormalities in presynaptic, rather than postsynaptic mechanisms (13). At a neurochemical level, presynaptic abnormalities of the machinery of neurosecretion may unify dopaminergic, glutamatergic and neurodevelopmental hypotheses (14; 15).

The intricate process of neurotransmitter release requires formation of the soluble N-ethylmaleimide-sensitive factor (NSF) attachment protein receptor (SNARE), a heterotrimeric complex assembled through the interaction of syntaxin-1 (Stx1), synaptosomal-associated protein-25 (SNAP25), and the vesicle-associated membrane protein (VAMP, or synaptobrevin) (16; 17). Although SNARE proteins are sufficient for *in vitro* vesicle priming and fusion (18), release of neurotransmitters is a highly regulated process requiring participation of multiple accessory proteins. In presynaptic membranes, vesicles are initially primed through a “trans-SNARE complex”, a partially assembled multimeric structure involving the additional participation of at least syntaxin-binding protein-1 (herein Munc18-1), complexin (Cplx) 1 or 2, and the calcium-sensitive protein synaptotagmin (Stg) (19-23). Calcium influx triggers the transition to a tight “cis-SNARE complex”, supplying the energy required to zipper vesicular and terminal membranes, and opening a fusion pore for neurotransmitter release (17; 24; 25). Finally, addition of NSF and soluble NSF attachment proteins (SNAP) to cis-SNAREs induces complex disassembly and vesicle recycling. A subset of dimeric SNARE associations, including target (t)-SNAREs (Stx1-SNAP25), is generated while the trans-SNAREs are rebuilt (17; 19).

Postmortem brain and gene association studies in schizophrenia consistently report abnormalities of individual components of the SNARE machinery (26-33), although there is no obvious convergence of findings across studies (26-30; 34-36). Compensatory *in vivo* effects related to SNARE functional efficiency (with or without altered expression of protein amounts) could be part of the pathological substrate of schizophrenia. For example, two murine strains carrying genetic modifications resulting in enhanced SNARE assembly (without obvious effect on expression levels of individual SNARE proteins) show schizophrenia-related endophenotypes. The ‘blind-drunk’ mouse bears a spontaneous

missense mutation in the SNAP25 gene, resulting in a single amino acid substitution (I67E) that confers enhanced SNARE binding affinity (37). Mutant mice showed higher vulnerability to a prenatal stress-induced schizophrenia-like syndrome, a behavioral manifestation that was abolished with antipsychotic treatment (38). More recently, transgenic mice overexpressing the accessory protein Munc18-1 were found to mimic structural and functional abnormalities present in schizophrenia patients, as well as showing enhanced dopamine release and behavioral activation with amphetamine (39). Conversely, impairment of SNARE proteins' capacity to form complexes was associated with cognitive decline and progression of Alzheimer's disease in a community-based aging study (40; 41), regardless of the amounts of Stx1 and SNAP25 present. Murine models mimicking the loss of SNARE protein-protein interactions undergo related behavioral and physiological neurodegenerative syndromes (42; 43). Finally, increased SNARE function could underlie the enhanced global brain signal recently observed by functional MRI in a large sample of patients with schizophrenia, a specific trait of illness that is mimicked by ketamine administration in healthy subjects (44; 45).

The unusual resistance of SNARE complexes to denaturation by sodium dodecyl sulfate (SDS) allows quantitation by standard SDS-polyacrylamide gel electrophoresis (PAGE) and Western blotting (46). However, whether all SNARE interactions are SDS-resistant, or only a subgroup of them (such as tight cis-SNAREs) is not known. Notably, SDS-resistant SNAREs were increased in cortical samples of schizophrenia suicides (28), but downregulated in antipsychotic-medicated subjects (30) and in schizophrenia samples with a large deficit in phosphoserine-14-Stx1 (35). In a previous study, increased native Stx1-SNAP25 interactions were identified in the ventromedial caudate nucleus of non-suicide schizophrenia samples by a modified sandwich ELISA (36). This technique, like co-immunoprecipitation (IP), cannot differentiate heterotrimeric from dimeric SNARE interactions. Separation of brain proteins in native gels, such as blue native (BN)-PAGE, may provide new insights into the structural and functional features of SNARE and other presynaptic complexes in both healthy and diseased brain. Unlike SDS-gels, BN-PAGE allows isolation of protein complexes while preserving their native conformations (47; 48). Quantitation of native SNARE interactions could represent a neurochemical indicator of synaptic activity.

We tested the hypothesis that SNARE function is enhanced in schizophrenia brain. Core SNARE protein-protein interactions were quantified in the orbitofrontal (OFC) and the anterior cingulate (ACC) cortices of a well-characterized postmortem series of schizophrenia subjects and matched controls. The findings were confirmed in a replication series of postmortem OFC samples. Relevant protein-protein interactions involving Munc18-1, Cplx1/2 and Stg, were also explored. Analyses of presynaptic protein-protein interactions involved two different quantitative assays: co-IP and BN-PAGE. Since this study is the first use of BN-PAGE to identify presynaptic complexes, additional *in vitro/ex vivo* assays were designed to better understand the functional relevance of the SNARE protein-protein interactions, including protein dephosphorylation and selective SNARE disruption with the chemical agent myricetin (49; 50).

## Methods and Materials

### Human postmortem brains

For the main, prospective study (Cohort 1), samples were obtained from the Macedonian/New York State Psychiatric Institute Brain Collection (36). Demographic and toxicological data of subjects with schizophrenia ( $n = 15$ ) and matched controls ( $n = 13$ ) are summarized in Tables S1 and S2 (see Supplement 1). Postmortem intervals (PMI) for all samples were relatively short compared to other available human cohorts (51), with controls (mean  $16.6 \pm \text{SD } 7.1$  hr) having slightly, but statistically significantly longer mean PMI than schizophrenia cases ( $8.8 \pm 3.4$  hr). Multiple investigations were conducted to investigate the possibility that postmortem factors or drug treatment could contribute to differences between schizophrenia and comparison samples (see Supplement 1). Grey matter samples from the OFC [Brodmann area (BA) 10/47] and ACC (BA 24) were dissected using a standard atlas (52), and homogenized as indicated in Supplement 1. Both OFC and ACC contribute to cognitive dysfunction in schizophrenia (53-56). The OFC was chosen for all prospective assays; the ACC was selected to address the possibility of regionally specific findings. A second series of OFC postmortem samples (Cohort 2) was obtained from the Stanley Foundation Neuropathology Consortium for replication, including 15 schizophrenia and 15 control donors (Supplementary Tables S1 and S3), with further details described elsewhere (57; 58).

### Animals, drug treatments, and *ex vivo* chemical manipulations

Treatment of rats with haloperidol and clozapine was as described (36, and Supplement 1). Control rat brain samples were additionally used in studies characterizing the effects of alkaline phosphatase (49) and selective myricetin-induced disruption (50) on SNARE protein-protein associations (Supplement 1).

### Co-IP, SDS-/BN-PAGE, and immunoblotting procedures

Detailed descriptions of these immunoassays and the antibodies used are provided in Supplement 1.

### Data analysis and statistics

As noted above, the primary hypothesis was that SNARE protein-protein interactions are increased in schizophrenia. We used complementary assays to provide converging tests of this hypothesis, including immunoprecipitation and BN-PAGE. A Gaussian distribution of final datasets was confirmed with the Kolmogorov-Smirnov normality test. Analyses of relationships between neurochemical measures and potential confounding variables (including PMI, age at death, gender, brain pH, sample storage time, presence of antipsychotics, benzodiazepines, and/or ethanol, and/or smoking habit) were carried out. In the absence of relationships with potential confounds, the primary analysis for comparisons between diagnostic groups (schizophrenia, control) was a *t*-test. Analyses of covariance (ANCOVA) were carried out when neurochemical findings showed an association with a potentially confounding variable. Pearson's correlations were used to inspect putative associations between SNARE protein-protein interactions and other exploratory findings

(such as measures of additional complexes), and to provide converging support for the primary hypothesis, or as exploratory analyses to be replicated in future studies. In animal studies, to assess possible effects of antipsychotic drugs, multiple comparisons were performed using one-way analysis of variance (ANOVA), followed by Bonferroni's *post-hoc* test. All tests were two-tailed, with statistical significance set to  $\alpha=.05$ . All data were analyzed with JMP, version 10.0.2 (SAS Institute, Cary, NC, USA), and graphs were plotted using GraphPad Prism 6.0a (GraphPad Software, La Jolla, CA, USA).

## Results

### Inspection of datasets and relationships with potentially confounding variables

All data series obtained in the neurochemical assessments were normally distributed. Except for PMI, no relevant associations were found between potentially confounding variables (age at death, gender, brain pH, sample storage time, presence of antipsychotics, benzodiazepines, and/or ethanol, and/or smoking habit) and the neurochemical findings. Since schizophrenia and control subjects within Cohort 1 differ statistically in mean PMI (Supplementary Table S1), multiple approaches were used to investigate possible effects of PMI that could complicate analyses related to diagnostic group (Supplement 1). These included (1) analysis of consistency of relationships with PMI across brain regions in the same cases, (2) analysis of consistency of relationships with PMI in an independent cohort (with no mean difference in PMI between diagnostic groups), (3) modeling PMI effects in a separate human postmortem brain series, and (4) using an ANCOVA model with PMI as a covariate. Additionally, possible effects of antipsychotic drugs were assessed in rats. Details of these investigations are provided in Supplement 1. Since there was no indication any of these alternate approaches resulted in different conclusions concerning the effects of diagnostic group, the statistical findings using direct comparisons without covariate(s) are presented below.

### Increased SNAP25 co-IP products in schizophrenia OFC with unaltered amounts in total homogenates

All SNARE proteins, as well as the binding partners Cplx1/2, Munc18-1 and Stg, were co-immunoprecipitated by anti-Stx1 and anti-SNAP25 antibodies (Figure 1A). The amount of co-IP product was linearly dependent on the total protein content in the sample (Figure 1B).

In total homogenates from the OFC (BA 10/47) in Cohort 1, densitometric analyses of SNAP25, Stx1, VAMP, Munc18-1, Cplx1/2, and Stg immunoblots showed no significant differences between schizophrenia samples and controls (Figure 1C). Similar negative results were observed in the ACC (BA 24) of the same subjects, and in the OFC in Cohort 2 (data not shown). In SNAP25-IP products from the OFC of Cohort 1, minimal variability of SNAP25 density was observed, and no mean differences were identified between groups (Figure 1D). However, the amount of Stx1 co-immunoprecipitating with SNAP25 was markedly greater in schizophrenia (+98%,  $p < .001$ ). The enhanced SNAP25-Stx1 interaction was not accompanied with increased VAMP association. Anti-SNAP25 IP extractions were also enriched in Munc18-1 (+113%,  $p < .05$ ) and Cplx1 (+118%,  $p < .01$ ) in schizophrenia OFC, contrasting with no differences in Cplx2 and Stg levels between the

groups (Figure 1D). These findings were not changed when using PMI as a covariate (see Supplementary Table S5).

### Identification of presynaptic complexes by 1-D/2-D BN/SDS-PAGE

One-dimensional (1-D) BN-PAGE separation of human cortical protein complexes (S1 fraction) followed by immunoblotting revealed a major band of ~150 kDa consistently immunolabeled with nine antibodies against Stx1, SNAP25, or VAMP (Figure 2A and Supplementary Figure S1), putatively corresponding to native SNARE. This complex was immunoprecipitated by anti-Stx1 and anti-SNAP25 and cross-detected with all antibodies against SNARE proteins (Supplementary Figure S2A). Additionally, other complexes (including a 200-kDa band) were observed above 150 kDa and up to 1.2 MDa, possibly corresponding to SNARE associations with other presynaptic multimeric structures (e.g. NSF, SNAPs). A SNAP25-VAMP complex of ~70 kDa was also recognized (and/or immunoprecipitated) with anti-SNAP25 and anti-VAMP, but not with anti-Stx1 (Figure 2 and Supplementary Figure S2).

To further characterize native SNAREs, brain samples were subjected to thermal and/or chemical denaturation (Figure 2A and Supplementary Figure S1). Surprisingly, in absence of SDS, heat did not disrupt the 150-kDa SNARE complex, but did dissociate multimeric complexes. Rapid *in vitro* reassembly during the assay may mask SNARE denaturation after boiling (61). SDS alone largely (but not fully) disrupted the 150-kDa SNARE complex, but was unable to disassemble the SNARE multimers. Combined, thermochemical denaturation resulted in full loss of SNARE complexes, with the consequent accumulation of monomeric forms.

In 2-D BN/SDS-PAGE, SNARE antibodies recognized a SDS-resistant, boiling-sensitive 75-kDa spot (Figure 2B and Supplementary Figure S3B), derived from the 150-kDa SNARE. The 70-kDa SNAP25-VAMP complex yielded a ~60-kDa spot, labeled with anti-SNAP25 and anti-VAMP, but not anti-Stx1 antibodies.

Exposure of solubilized protein complexes to alkaline phosphatase and myricetin revealed functional features of the native 150-kDa SNARE complex. Enzymatic dephosphorylation induced a shift of molecular mass to 200 kDa, apparently caused by the attachment of Cplx1 (Figure 3A; Supplement 1). This effect was not observed in SDS-gels (Figure 3B). Moreover, upon removal of phosphate groups, Stx1-IP samples were significantly enriched in Munc18-1, Cplx2 and Stg (+65-182%), which did not interfere with SNARE intrinsic interactions (Figure 3C). The SNARE complex inhibitor myricetin disrupted the 150-kDa complex in a concentration-dependent manner ( $IC_{50} = .3-.6 \mu M$ ,  $p < .001$ ), without altering total contents of Stx1, SNAP25 and VAMP (Figure 3D). These experiments show that BN-, rather than SDS-PAGE, is sensitive to qualitative and quantitative changes in SNARE associations.

### Altered patterns of native presynaptic protein complexes in schizophrenia OFC and ACC

The immunodensities of SNARE and other presynaptic complexes in the OFC (BA 10/47) and/or the ACC (BA 24) of subjects from Cohorts 1 and 2 were assessed by 1-D BN-PAGE

followed by standard immunoblotting with antibodies against Stx1, SNAP25, VAMP, Cplx1 and Stg. As a test of the primary hypothesis of increased SNARE interaction, the mean value for immunoreactivity of the 150-kDa SNARE complex was found to be increased in the OFC of schizophrenia samples (+45%,  $p = .0009$ ), consistent across each of the three immunolabeled SNARE proteins (+34-53%,  $p = .0006-.0095$ , Figure 4A, upper panel). Similar upregulation of the mean immunolabelling of the 150-kDa SNARE complex was observed in the ACC of the same schizophrenia subjects (+44%,  $p = .0307$ ), with converging, statistically significant findings for quantification with the anti-Stx1 (+50%,  $p = .0195$ ), and anti-SNAP25 antibodies (+39%,  $p = .0452$ ), but not the anti-VAMP antibody (+42%,  $p = .0546$ , Figure 4A, middle panel). Consistent findings were obtained in a replication study analyzing samples from the OFC (BA 10/47) of subjects from Cohort 2 (Figure 4A, bottom panel). SNARE associations were significantly enhanced for the mean immunolabelling (+44%,  $p = .0002$ ), and for each of the three anti-SNARE antibodies (+31-54%,  $p = .0266-.0002$ ). Remarkably, when PMI was included in ANCOVA for the Cohort 1 OFC samples, diagnosis [ $F(1,24) = 11.327$ ;  $p = .0026$ ], but not PMI [ $F(1,24) = 0.5305$ ;  $p = 0.4734$ ], accounted for the vast variability explained by the model (see also Supplementary Table S5). Correlations between the three measurements of SNARE complex immunoreactivity were highly significant (Figure 4C), indicating that changes in SNARE complex levels can be reliably detected with Stx1, SNAP25 or VAMP antibodies.

The putative ~70-kDa SNAP25-VAMP complex could only be quantified in SNAP25 immunoblots, since detection with anti-VAMP antibody resulted in a weak and more diffuse band (see Figure 2A). Lower density (-37%,  $p < .05$ ) of this complex was observed in the OFC of subjects with schizophrenia in Cohort 1 (Figure 4B, upper panel). The putative SNARE-Cplx1 structure observed at 200-kDa was at higher levels in the same schizophrenia samples (+65%,  $p < .05$ ), whereas the 550-kDa Cplx1 containing complex was slightly lower (24%,  $p > .05$ ) (Figure 4B, upper panel). However, these secondary alterations of the presynaptic protein interactome were not observed in the ACC of the same subjects, or in the OFC of schizophrenia group in Cohort 2, compared to their matched controls (Figure 4B, middle and bottom panels). Interestingly, the cortical level of 200-kDa Cplx1 was strongly associated with that of 150-kDa SNARE complex in both regions and cohorts (Figure 4C, right panel), suggesting a cooperative interaction between these complexes. Of the Stg complexes, only the 350-kDa complex was measurable in control and schizophrenia samples, while the 130-kDa complex was barely detectable. No significant differences in the large Stg complex were observed between the groups in any of the regions analyzed in Cohort 1 (Figure 4B), so no further replication was assessed in Cohort 2.

### **Converging evidence across techniques supports presynaptic alterations in schizophrenia OFC**

As expected, pairwise analyses across immunological techniques (Table 1) showed a significant correlation between the amounts of SNAP25-immunoprecipitated Stx1 and those of native 150-kDa SNARE complex, quantified in the OFC of subjects with schizophrenia and controls in Cohort 1. This SNAP25-Stx1 interaction was negatively correlated with the putative 70-kDa SNAP25-VAMP dimer, suggesting a dynamic conversion between 150-kDa and 70-kDa species, that is unbalanced in schizophrenia. Accordingly, no significant

associations were found between these species and the VAMP co-IP product, which remains attached in both complexes. Remarkably, positive correlations were also detected between Munc18-1 and Cplx1 co-IP products and the ~150-kDa SNARE, which suggest a cooperative action of these accessory proteins on the enhanced SNARE interactions in schizophrenia brain. Consistent with complex transformations, significant associations were observed between the cortical immunodensities of Cplx1-SNAP25 co-IP, and those of native Cplx1 oligomers of ~200 kDa (positive) and ~550 kDa (negative). Immunoprecipitated Munc18-1 was also largely related to the ~200-kDa SNARE-Cplx1 oligomer, suggesting a role in building this complex. Individual protein densities in total homogenates, as well as the contents of Cplx2 and Stg in SNAP25-IP products, did not show significant correlations with the presynaptic complexes quantified in native gels. Note, however, that co-IP experiments were not reassessed in ACC or in the replication study with Cohort 2 due to limitations on sample availability.

### Modeling effects of PMI and antipsychotic drugs

An independent series of controls selected for a similar range of PMI (7-25 h) was studied, as well as an investigation of the possible effects of typical (haloperidol) or atypical (clozapine) antipsychotics on cortical SNARE complex in rats. In summary, none of these variables appeared to explain the abnormal SNARE protein-protein interactions observed in schizophrenia (see Supplement 1 and Figures S5 and S6 therein).

### Discussion

The present study explored the diversity of interactions of SNARE proteins (Stx1, SNAP25 and VAMP) and relevant presynaptic binding partners (Munc18-1, Cplx1/2, Stg) with two different immunoassay strategies (co-IP and BN-PAGE). Schizophrenia was associated with greater OFC and ACC SNARE complex formation, without alteration in protein expression levels. Greater Cplx1 and/or Munc18-1 binding affinity may underlie the aberrant SNARE complex formation in schizophrenia.

Native gels were used for comprehensive characterization of presynaptic complexes. In 1-D BN-PAGE, the SNARE complex was resolved as a 150-kDa major structure. Despite the resistance of SNARE interactions to SDS-PAGE denaturing conditions (30; 46; 61), native 150-kDa SNARE complexes showed high sensitivity to SDS in BN-PAGE. This divergent behavior may represent two different pools of SNARE complexes, corresponding to the partially zippered trans-SNAREs (SDS-sensitive), and the tight cis-SNAREs (SDS-resistant) (23). The high sensitivity of native 150-kDa SNARE to enzymatic dephosphorylation and myricetin-induced disruption may reflect the functionality of these complexes (50; 62). The theoretical weight of SNARE heterotrimer (Stx1+SNAP25+VAMP) is only 74 kDa, suggesting additional binding partner(s) may be present in the 150 kDa native complex. Munc18-1 is a strong candidate, supported by its profile in 2-D BN-blots and the predicted weight (142 kDa) of the existing SNARE-Munc18 tetramer (19-22). Two other SNARE species were characterized: a 200-kDa complex containing SNARE proteins and Cplx1 (and putatively Munc18-1), and a 70-kDa SNAP25-VAMP dimer. These protein complexes were confirmed by both 2-D BN/SDS-PAGE and co-IP assays. While SNARE-Cplx1 oligomers



were expected (63; 64), SNAP25-VAMP dimers were a surprise. In SNARE assembly, t-SNAREs (Stx1-SNAP25) are formed first, and v-SNAREs (VAMP) are attached later (61). This binary interaction could be a transient product resulting from NSF-mediated SNARE dissociation (61; 65). Other SNARE-containing multimeric complexes of higher molecular weight (250-1200 kDa) were detected, and require further characterization in future studies using mass spectroscopy to allow identification of all components of the complexes.

For schizophrenia, the findings indicate upregulated OFC and ACC SNARE complex formation. Although the immunodensities of SNARE monomers, Munc18-1, Cplx1/2 or Stg in total homogenates were not different from control levels, IP studies showed increased SNAP25-Stx1 interaction in schizophrenia, without a significant alteration in SNAP25-VAMP association. In parallel, using BN-PAGE, the 150-kDa complex was increased in the same brain samples, regardless of the SNARE protein targeted, while the putative SNAP25-VAMP dimer was reduced. Immunoprecipitation studies showed enhanced SNAP25 binding affinity for Munc18-1 and Cplx1 in schizophrenia brains, correlating positively with the upregulated 200-kDa SNARE-Cplx1 oligomer, and negatively with 550-kDa Cplx1 multimer. The correlations across both techniques (see Table 1), combined with key findings in the literature, suggest dynamic conversion or partitioning of SNARE and related proteins between these complexes, which in turn may underlie cycling of presynaptic vesicles (schematically represented in Figure 5). Since protein associations likely occur *in vitro* during the assays (46), the increased efficiency of formation of active SNARE protein complexes suggests that turnover within the proposed cycle may be accelerated in schizophrenia. Importantly, the upregulated 150-kDa SNARE complex in the OFC and the ACC of Cohort 1 was confirmed in Cohort 2, despite large demographic and recent treatment differences between cohorts that could potentially mask the intrinsic biological mechanisms of illness in postmortem studies. Other exploratory observations in the OFC in Cohort 1 were not replicated in the ACC or in Cohort 2. These latter findings, involving Cplx1 and other SNARE associations resolved by BN-PAGE, might be sensitive to the confounding variables described above, could be region specific, and/or inconsistently part of the illness.

Alterations in both mRNA and protein expression levels of neurosecretory molecules have long been reported in schizophrenia postmortem brain, including increased levels of Stx1 and/or reduced SNAP25 (15; 66). In agreement with the present data, one study showed upregulated native SNAP25-Stx1 interaction in ventromedial caudate samples in schizophrenia (36). Phosphorylation of SNARE proteins and their binding partners is crucial for SNARE efficiency, with some phosphorylation sites stimulating and others repressing complex formation (62). In the present study, *ex vivo* removal of phosphate groups did not alter intrinsic SNARE interactions, indicating that a homeostatic balance between phospho-stimulator and phospho-repressor sites is achieved in presynaptic terminals. However, full phosphate depletion promoted adhesion of Munc18-1, Cplx1/2 and Stg to the complex. Of note, previous postmortem studies found higher Munc18-1 levels in schizophrenia dorsolateral prefrontal cortex, that were reduced by chronic antipsychotic medication (30; 67). These observations suggest that a new homeostatic state involving dysregulated phospho-stimulator/repressor sites could result in a higher efficiency of SNARE complex

association in schizophrenia (Figure 5). Notably, the findings are convergent with ‘blind-drunk’ and Munc18-1-overexpressing mice models, both displaying enhanced SNARE interactions and schizophrenia-related behaviors (38; 39). It remains uncertain whether or not the antipsychotic-induced amelioration of the schizophrenia-like endophenotypes in these murine models is mediated by normalization of the intrinsically elevated SNARE protein-protein interactions.

The present findings indicated a role of Cplx1 (but not Cplx2) in the enhanced SNARE function in schizophrenia OFC. Cplx1 is mainly expressed in inhibitory neurons, while excitatory terminals are enriched in Cplx2 (63; 64). Orbitofrontal GABAergic, but not glutamatergic neurons may display aberrant SNARE complex activity, which could result in constitutive inhibition of the glutamate system, and perhaps contribute to lower OFC function (8). Interestingly, reduced OFC activity (quantified by functional MRI) is associated with poor executive functioning in patients with schizophrenia (53; 54). Since Cplx1 oligomers were not altered in the ACC, increased SNARE function in this region might not be associated with inhibitory terminals. Co-IP experiments may determine whether increased Cplx2 binding mediates enhanced SNARE association in ACC, putatively involving excitatory terminals. Future studies characterizing the functional and structural profiles of the diverse complexes observed in native gels, and their potential association with specific terminal subtypes, may allow tracing SNARE complex alterations in excitatory, inhibitory and/or neuromodulatory synaptic terminals across different brain regions. Illness specificity also requires attention in future studies. In this context, previous work showed no association between major depression and SDS-resistant complexes (30), while another study reported a positive association between disturbed native SNARE interactions and age-related cognitive impairment (40).

In conclusion, the present findings indicate enhanced cortical SNARE protein-protein interactions in schizophrenia. The putative upregulated SNARE function may be facilitated by increased affinity for Cplx1 and/or Munc18-1. Research on novel drugs to treat the core biochemical mechanisms of schizophrenia could seek compounds capable of disrupting SNARE complex association.

## Supplementary Material

Refer to Web version on PubMed Central for supplementary material.

## Acknowledgements

The study was supported by the Canadian Institutes of Health Research (MT-14037, MOP-81112) and the Michael Smith Foundation for Health Research, the National Institute of Mental Health (MH60877, MH64168, MH62185, MH45212, MH64673), NARSAD, and the Lieber Center for Schizophrenia Research. AR-M is a Post-Doctoral Fellow supported by Michael Smith Foundation for Health Research and BC Schizophrenia Society Foundation. We thank Hong-Ying Li and Vilte E Barakauskas for their skillful assistance.

Dr. Honer has received consulting fees or sat on paid advisory boards for: MDH Consulting, In Silico, Otsuka/Lundbeck, Eli Lilly and Roche. Dr. Barr is on the advisory board or received consulting fees from Roche Canada, and received educational grant support from BMS Canada. Dr. Mann receives royalties from the Research Foundation for Mental Hygiene for commercial use of the C-SSRS and has stock options in Qualitas Health a start-up developing a PUFA supplement.

## References

1. Jablensky A. The 100-year epidemiology of schizophrenia. *Schizophr Res.* 1997; 28:111–125. [PubMed: 9468347]
2. McGrath J, Saha S, Chant D, Welham J. Schizophrenia: a concise overview of incidence, prevalence, and mortality. *Epidemiol Rev.* 2008; 30:67–76. [PubMed: 18480098]
3. Carlsson ML, Carlsson A, Nilsson M. Schizophrenia: from dopamine to glutamate and back. *Curr Med Chem.* 2004; 11:267–277. [PubMed: 14965231]
4. Harrison PJ, Weinberger DR. Schizophrenia genes, gene expression, and neuropathology: on the matter of their convergence. *Mol Psychiatry.* 2005; 10:40–68. [PubMed: 15263907]
5. Paz RD, Tardito S, Atzori M, Tseng KY. Glutamatergic dysfunction in schizophrenia: From basic neuroscience to clinical psychopharmacology. *Eur Neuropsychopharmacol.* 2008; 18:773–786. [PubMed: 18650071]
6. Heinz A, Schlagenhauf F. Dopaminergic dysfunction in schizophrenia: salience attribution revisited. *Schizophr Bull.* 2010; 36:472–485. [PubMed: 20453041]
7. Lisman JE, Pi HJ, Zhang Y, Otmakhova NA. A Thalamo-Hippocampal-Ventral Tegmental Area Loop May Produce the Positive Feedback that Underlies the Psychotic Break in Schizophrenia. *Biol Psychiatry.* 2010; 68:17–24. [PubMed: 20553749]
8. Marek GJ, Behl B, Beshpalov AY, Gross G, Lee Y, Schoemaker H. Glutamatergic (N-methyl-D-aspartate receptor) hypofrontality in schizophrenia: too little juice or a miswired brain? *Mol Pharmacol.* 2010; 77:317–326. [PubMed: 19933774]
9. Weinberger DR. Implications of normal brain development for the pathogenesis of schizophrenia. *Arch Gen Psychiatry.* 1987; 44:660–669. [PubMed: 3606332]
10. Benes FM. Model generation and testing to probe neural circuitry in the cingulate cortex of postmortem schizophrenic brain. *Schizophr Bull.* 1998; 24:219–230. [PubMed: 9613622]
11. Arnold SE. Cognition and neuropathology in schizophrenia. *Acta Psychiatr Scand Suppl.* 1999; 395:41–50. [PubMed: 10225332]
12. Stephan KE, Friston KJ, Frith CD. Dysconnection in schizophrenia: from abnormal synaptic plasticity to failures of self-monitoring. *Schizophr Bull.* 2009; 35:509–527. [PubMed: 19155345]
13. Howes OD, Kambaitz J, Kim E, Stahl D, Slifstein M, Abi-Dargham A, Kapur S. The nature of dopamine dysfunction in schizophrenia and what this means for treatment. *Arch Gen Psychiatry.* 2012; 69:776–786. [PubMed: 22474070]
14. Karson CN, Mrak RE, Schluterman KO, Sturmer WQ, Sheng JG, Griffin WS. Alterations in synaptic proteins and their encoding mRNAs in prefrontal cortex in schizophrenia: a possible neurochemical basis for “hypofrontality”. *Mol Psychiatry.* 1999; 4:39–45. [PubMed: 10089007]
15. Johnson RD, Oliver PL, Davies KE. SNARE proteins and schizophrenia: linking synaptic and neurodevelopmental hypotheses. *Acta Biochim Pol.* 2008; 55:619–628. [PubMed: 18985177]
16. Söllner T, Whiteheart SW, Brunner M, Erdjument-Bromage H, Geromanos S, Tempst P, Rothman JE. SNAP receptors implicated in vesicle targeting and fusion. *Nature.* 1993; 362:318–324. [PubMed: 8455717]
17. Sollner T, Bennett MK, Whiteheart SW, Scheller RH, Rothman JE. A protein assembly-disassembly pathway in vitro that may correspond to sequential steps of synaptic vesicle docking, activation, and fusion. *Cell.* 1993; 75:409–418. [PubMed: 8221884]
18. Weber T, Zemelman BV, McNew JA, Westermann B, Gmachl M, Parlati F, et al. SNAREpins: Minimal machinery for membrane fusion. *Cell.* 1998; 92:759–772. [PubMed: 9529252]
19. Rizo J, Südhof TC. Snares and Munc18 in synaptic vesicle fusion. *Nat Rev Neurosci.* 2002; 3:641–653. [PubMed: 12154365]
20. Verhage M, Toonen RF. Regulated exocytosis: merging ideas on fusing membranes. *Curr Opin Cell Biol.* 2007; 19:402–408. [PubMed: 17629692]
21. Rizo J, Rosenmund C. Synaptic vesicle fusion. *Nat Struct Mol Biol.* 2008; 15:665–674. [PubMed: 18618940]
22. Südhof TC, Rothman JE. Membrane fusion: grappling with SNARE and SM proteins. *Science.* 2009; 323:474–477. [PubMed: 19164740]

23. Südhof TC. Neurotransmitter release: the last millisecond in the life of a synaptic vesicle. *Neuron*. 2013; 80:675–690. [PubMed: 24183019]
24. Gerber SH, Rah J-C, Min S-W, Liu X, de Wit H, Dulubova I, et al. Conformational switch of syntaxin-1 controls synaptic vesicle fusion. *Science*. 2008; 321:1507–1510. [PubMed: 18703708]
25. Deák F, Xu Y, Chang W-P, Dulubova I, Khvotchev M, Liu X, et al. Munc18-1 binding to the neuronal SNARE complex controls synaptic vesicle priming. *J Cell Biol*. 2009; 184:751–764. [PubMed: 19255244]
26. Gabriel SM, Haroutunian V, Powchih P, Honer WG, Davidson M, Davies P, et al. Increased concentrations of presynaptic proteins in the cingulate cortex of subjects with schizophrenia. *Arch Gen Psychiatry*. 1997; 54:559–566. [PubMed: 9193197]
27. Honer WG, Falkai P, Young C, Wang T, Xie J, Bonner J, et al. Cingulate cortex synaptic terminal proteins and neural cell adhesion molecule in schizophrenia. *Neuroscience*. 1997; 78:99–110. [PubMed: 9135092]
28. Honer WG, Falkai P, Bayer TA, Xie J, Hu L, Li H-Y, et al. Abnormalities of SNARE mechanism proteins in anterior frontal cortex in severe mental illness. *Cereb Cortex*. 2002; 12:349–356. [PubMed: 11884350]
29. Sokolov BP, Tcherepanov AA, Haroutunian V, Davis KL. Levels of mRNAs encoding synaptic vesicle and synaptic plasma membrane proteins in the temporal cortex of elderly schizophrenic patients. *Biol Psychiatry*. 2000; 48:184–196. [PubMed: 10924661]
30. Gil-Pisa I, Munarriz-Cuezva E, Ramos-Miguel A, Urigüen L, Meana JJ, García-Sevilla JA. Regulation of munc18-1 and syntaxin-1A interactive partners in schizophrenia prefrontal cortex: down-regulation of munc18-1a isoform and 75 kDa SNARE complex after antipsychotic treatment. *Int J Neuropsychopharmacol*. 2012; 15:573–588. [PubMed: 21669024]
31. Wong AHC, Trakalo J, Likhodi O, Yusuf M, Macedo A, Azevedo MH, et al. Association between schizophrenia and the syntaxin 1A gene. *Biol Psychiatry*. 2004; 56:24–29. [PubMed: 15219469]
32. Fanous AH, Zhao Z, van den Oord EJCG, Maher BS, Thiselton DL, Bergen SE, et al. Association study of SNAP25 and schizophrenia in Irish family and case-control samples. *Am J Med Genet B Neuropsychiatr Genet*. 2010; 153B:663–674. [PubMed: 19806613]
33. Lochman J, Balcar VJ, Štastný F, Šerý O. Preliminary evidence for association between schizophrenia and polymorphisms in the regulatory Regions of the ADRA2A, DRD3 and SNAP-25 Genes. *Psychiatry Res*. 2013; 205:7–12. [PubMed: 22940547]
34. Halim ND, Weickert CS, McClintock BW, Hyde TM, Weinberger DR, Kleinman JE, Lipska BK. Presynaptic proteins in the prefrontal cortex of patients with schizophrenia and rats with abnormal prefrontal development. *Mol Psychiatry*. 2003; 8:797–810. [PubMed: 12931207]
35. Castillo MA, Ghose S, Tamminga CA, Ulery-Reynolds PG. Deficits in Syntaxin 1 Phosphorylation in Schizophrenia Prefrontal Cortex. *Biol Psychiatry*. 2010; 67:208–216. [PubMed: 19748077]
36. Barakauskas VE, Beasley CL, Barr AM, Ypsilanti AR, Li H-Y, Thornton AE, et al. A novel mechanism and treatment target for presynaptic abnormalities in specific striatal regions in schizophrenia. *Neuropsychopharmacology*. 2010; 35:1226–1238. [PubMed: 20072114]
37. Jeans AF, Oliver PL, Johnson R, Capogna M, Vikman J, Molnár Z, et al. A dominant mutation in Snap25 causes impaired vesicle trafficking, sensorimotor gating, and ataxia in the blind-drunk mouse. *Proc Natl Acad Sci U S A*. 2007; 104:2431–2436. [PubMed: 17283335]
38. Oliver PL, Davies KE. Interaction between environmental and genetic factors modulates schizophrenic endophenotypes in the Snap-25 mouse mutant blind-drunk. *Hum Mol Genet*. 2009; 18:4576–4589. [PubMed: 19729413]
39. Urigüen L, Gil-Pisa I, Munarriz-Cuezva E, Berrocoso E, Pascau J, Soto-Montenegro ML, et al. Behavioral, neurochemical and morphological changes induced by the overexpression of munc18-1a in brain of mice: relevance to schizophrenia. *Transl Psychiatry*. 2013; 3:e221. [PubMed: 23340504]
40. Honer WG, Barr AM, Sawada K, Thornton AE, Morris MC, Leurgans SE, et al. Cognitive reserve, presynaptic proteins and dementia in the elderly. *Transl Psychiatry*. 2012; 2:e114. [PubMed: 22832958]

41. Boyle PA, Wilson RS, Yu L, Barr AM, Honer WG, Schneider JA, Bennett DA. Much of late life cognitive decline is not due to common neurodegenerative pathologies. *Ann Neurol*. 2013; 74:478–489. [PubMed: 23798485]
42. Nakata Y, Yasuda T, Fukaya M, Yamamori S, Itakura M, Nihira T, et al. Accumulation of  $\alpha$ -synuclein triggered by presynaptic dysfunction. *J Neurosci*. 2012; 32:17186–17196. [PubMed: 23197711]
43. Sharma M, Burre J, Sudhof TC. Proteasome Inhibition Alleviates SNARE-Dependent Neurodegeneration. *Sci Transl Med*. 2012; 4:147ra113.
44. Yang GJ, Murray JD, Repovs G, Cole MW, Savic a, Glasser MF, et al. Altered global brain signal in schizophrenia. *Proc Natl Acad Sci*. 2014; 111:7438–7443. [PubMed: 24799682]
45. Driesen NR, McCarthy G, Bhagwagar Z, Bloch M, Calhoun V, D'Souza DC, et al. Relationship of resting brain hyperconnectivity and schizophrenia-like symptoms produced by the NMDA receptor antagonist ketamine in humans. *Mol Psychiatry*. 2013; 18:1199–1204. [PubMed: 23337947]
46. Hayashi T, McMahon H, Yamasaki S, Binz T, Hata Y, Südhof TC, Niemann H. Synaptic vesicle membrane fusion complex: action of clostridial neurotoxins on assembly. *EMBO J*. 1994; 13:5051–5061. [PubMed: 7957071]
47. Schagger H, Von Jagow G. Blue native electrophoresis for isolation of membrane protein complexes in enzymatically active form. *Anal Biochem*. 1991; 199:223–231. [PubMed: 1812789]
48. Wittig I, Braun H-P, Schägger H. Blue native PAGE. *Nat Protoc*. 2006; 1:418–428. [PubMed: 17406264]
49. Ramos-Miguel A, García-Fuster MJ, Callado LF, La Harpe R, Meana JJ, García-Sevilla JA. Phosphorylation of FADD (Fas-associated death domain protein) at serine 194 is increased in the prefrontal cortex of opiate abusers: relation to mitogen activated protein kinase, phosphoprotein enriched in astrocytes of 15 kDa, and Akt signaling pathways. *Neuroscience*. 2009; 161:23–38. [PubMed: 19303913]
50. Yang Y, Shin JY, Oh J-M, Jung CH, Hwang Y, Kim S, et al. Dissection of SNARE-driven membrane fusion and neuroexocytosis by wedging small hydrophobic molecules into the SNARE zipper. *Proc Natl Acad Sci U S A*. 2010; 107:22145–22150. [PubMed: 21135223]
51. Deep-Soboslay A, Benes FM, Haroutunian V, Ellis JK, Kleinman JE, Hyde TM. Psychiatric brain banking: Three perspectives on current trends and future directions. *Biol Psychiatry*. 2011; 69:104–112. [PubMed: 20673875]
52. Mai, JK.; Assheuer, J.; Paxinos, G. Atlas of the human brain. 3rd ed.. Academic Press; San Diego, CA: 1997.
53. Camchong J, Dyckman KA, Austin BP, Clementz BA, McDowell JE. Common neural circuitry supporting volitional saccades and its disruption in schizophrenia patients and relatives. *Biol Psychiatry*. 2008; 64:1042–1050. [PubMed: 18692173]
54. Goghari VM. Executive functioning-related brain abnormalities associated with the genetic liability for schizophrenia: an activation likelihood estimation meta-analysis. *Psychol Med*. 2011; 41:1239–1252. [PubMed: 20942994]
55. Dolan RJ, Fletcher P, Frith CD, Friston KJ, Frackowiak RS, Grasby PM. Dopaminergic modulation of impaired cognitive activation in the anterior cingulate cortex in schizophrenia. *Nature*. 1995; 378:180–182. [PubMed: 7477319]
56. Carter CS, Mintun M, Nichols T, Cohen JD. Anterior cingulate gyrus dysfunction and selective attention deficits in schizophrenia: [ $^{15}$ O]H $_2$ O PET study during single-trial Stroop task performance. *Am J Psychiatry*. 1997; 154:1670–1675. [PubMed: 9396944]
57. Beasley CL, Honer WG, Bergmann K, Falkai P, Lütjohann D, Bayer TA. Reductions in cholesterol and synaptic markers in association cortex in mood disorders. *Bipolar Disord*. 2005; 7:449–455. [PubMed: 16176438]
58. Torrey EF, Webster M, Knable M, Johnston N, Yolken RH. The stanley foundation brain collection and neuropathology consortium. *Schizophr Res*. 2000; 44:151–155. [PubMed: 10913747]

59. García-Fuster MJ, Ramos-Miguel A, Rivero G, La Harpe R, Meana JJ, García-Sevilla JA. Regulation of the extrinsic and intrinsic apoptotic pathways in the prefrontal cortex of short- and long-term human opiate abusers. *Neuroscience*. 2008; 157:105–119. [PubMed: 18834930]
60. Sapp E, Valencia A, Li X, Aronin N, Kegel KB, Vonsattel J-P, et al. Native mutant Huntingtin in human brain: Evidence for prevalence of full length monomer. *J Biol Chem*. 2012; 287:13487–13499. [PubMed: 22375012]
61. Fasshauer D, Otto H, Eliason WK, Jahn R, Brünger AT. Structural changes are associated with soluble N-ethylmaleimide-sensitive fusion protein attachment protein receptor complex formation. *J Biol Chem*. 1997; 272:28036–28041. [PubMed: 9346956]
62. Snyder DA, Kelly ML, Woodbury DJ. SNARE complex regulation by phosphorylation. *Cell Biochem Biophys*. 2006; 45:111–123. [PubMed: 16679567]
63. Takahashi S, Yamamoto H, Matsuda Z, Ogawa M, Yagyu K, Taniguchi T, et al. Identification of two highly homologous presynaptic proteins distinctly localized at the dendritic and somatic synapses. *FEBS Lett*. 1995; 368:455–460. [PubMed: 7635198]
64. Sawada K, Barr AM, Nakamura M, Arima K, Young CE, Dwork AJ, et al. Hippocampal complexin proteins and cognitive dysfunction in schizophrenia. *Arch Gen Psychiatry*. 2005; 62:263–272. [PubMed: 15753239]
65. Hayashi T, Yamasaki S, Nauenburg S, Binz T, Niemann H. Disassembly of the reconstituted synaptic vesicle membrane fusion complex in vitro. *EMBO J*. 1995; 14:2317–2325. [PubMed: 7774590]
66. Fung SJ, Sivagnanasundaram S, Weickert CS. Lack of change in markers of presynaptic terminal abundance alongside subtle reductions in markers of presynaptic terminal plasticity in prefrontal cortex of schizophrenia patients. *Biol Psychiatry*. 2011; 69:71–79. [PubMed: 21145444]
67. Behan AT, Byrne C, Dunn MJ, Cagney G, Cotter DR. Proteomic analysis of membrane microdomain-associated proteins in the dorsolateral prefrontal cortex in schizophrenia and bipolar disorder reveals alterations in LAMP, STXBP1 and BASP1 protein expression. *Mol Psychiatry*. 2009; 14:601–613. [PubMed: 18268500]

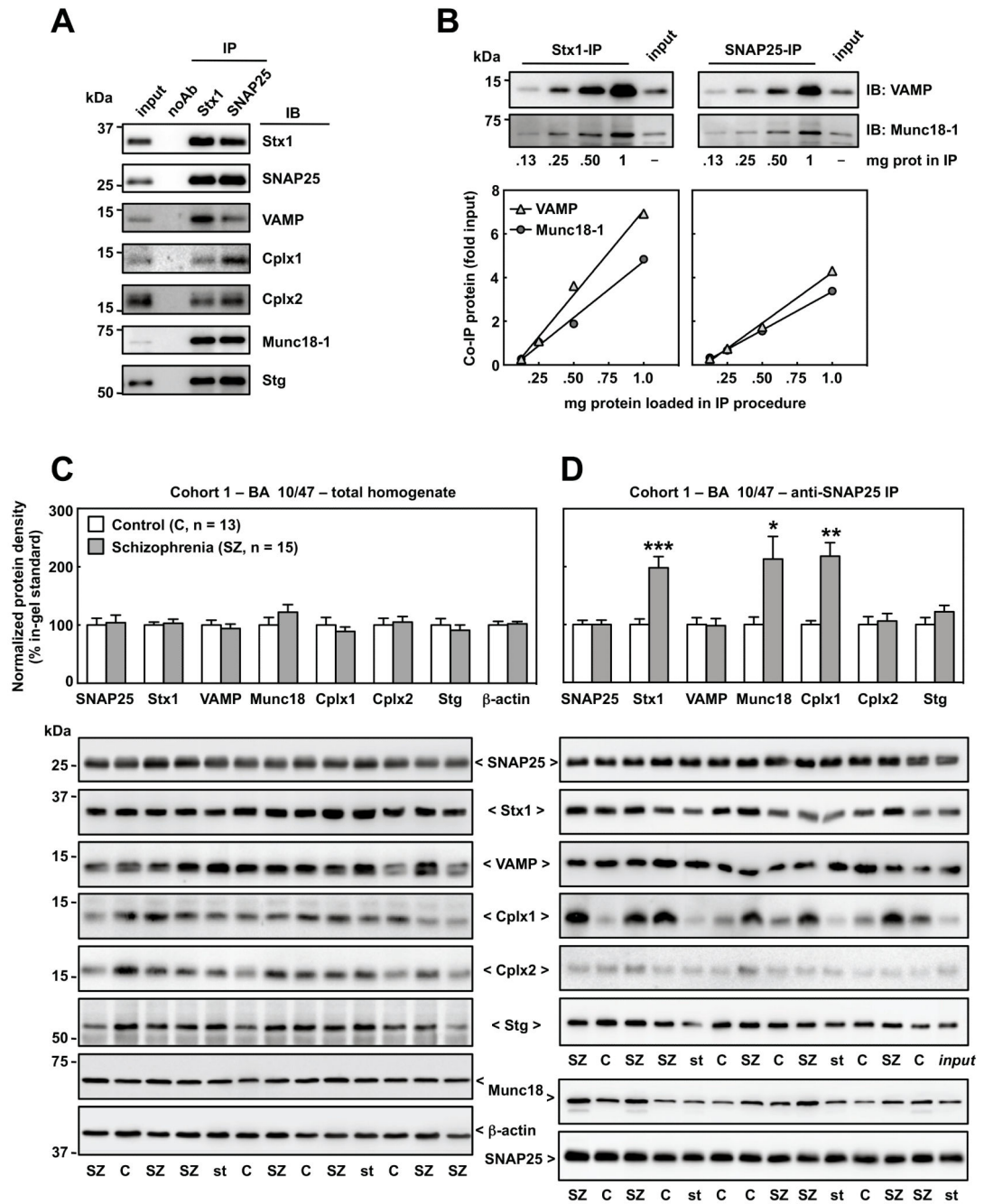


**Figure 1.**

Characterization and quantification of presynaptic protein-protein interactions in control and schizophrenia brain samples from the orbitofrontal cortex (OFC, BA 10/47) in Cohort 1 by standard immunoblotting (IB) and immunoprecipitation (IP). (A) Solubilized brain proteins (1 mg in 200 µl) were incubated with magnetic beads pre-coated in absence (noAb; negative control) or presence of antibodies against Stx1 (SP7) or SNAP25 (SP12), and eluted in 50 µl of SDS-loading buffer. Five µl of the resulting pellets, alongside 5 µg of IP input sample, were resolved by SDS-PAGE followed by IB with specific antibodies. VAMP, Cplx1/2,

Munc18-1 and Stg similarly co-immunoprecipitated either with anti-Stx1 or anti-SNAP25. For all tested antibodies, no immunoreactivity was detected in noAb sample, reflecting a high purity of the extraction procedure and the specificity of the protein-protein interactions. **(B)** Stx1 and SNAP25 were immunoprecipitated as above using as inputs increasing amounts (.13-1.0 mg) of human brain solubilized proteins. Pellets (5  $\mu$ l) and the input sample (5  $\mu$ g) were analyzed in SDS-PAGE followed by quantitative IB for two major co-IP products, VAMP and Munc18-1 (representative immunoblots on top). Immunodensities of each co-IP product in each IP reaction were calculated as the ratio to input value, and individually represented in the graphs against the protein concentration used in each IP procedure. Both co-IP products were linearly dependent on the total protein amount (and thereby in the amount of protein-protein interactions) loaded in both IP reactions with anti-Stx1 (VAMP:  $r = .996$ ,  $p = .0042$ ; Munc18-1:  $r = .995$ ,  $p = .005$ ) and anti-SNAP25 (VAMP:  $r = .997$ ,  $p = .0026$ ; Munc18-1:  $r = .999$ ,  $p = .0007$ ) antibodies, for the entire range of studied concentrations. **(C and D)** Altered presynaptic protein-protein interactions in schizophrenia OFC. Immunodensities of SNAP25, Stx1, VAMP, Munc18-1, Cplx1/2 and Stg were quantified in total brain homogenates **(C)** and in anti-SNAP25 (SP12) immunoprecipitation (IP) products **(D)** from the OFC of control and schizophrenia subjects in Cohort 1 ( $n = 13-15$ ). Values were normalized by  $\beta$ -actin **(C)** or SNAP25 **(D)** and represented (in bars) as mean  $\pm$  SEM percentage values from in-gel standards (pool of control samples); \* $p < .05$ , \*\* $p < .01$ , \*\*\* $p < .001$  (Student's  $t$ -test). Bottom **(C and D)**: representative immunoblots from various control (C), schizophrenia (SZ), standard (st) samples, and the input used for standard IP (*st input*). Note that selected immunoblots for all proteins (excluding Munc18-1-co-IP) correspond to the same subsets of C and SZ subjects identically distributed across the gels. The equivalent gel for Munc18-1 **(D)** was anomalous and another representative immunoblot was selected. The images were developed by a researcher blind to the identity of the samples **(A-D)** Mass (in kDa) of the most proximal prestained protein marker (Bio-Rad) to the target proteins is indicated on the left.



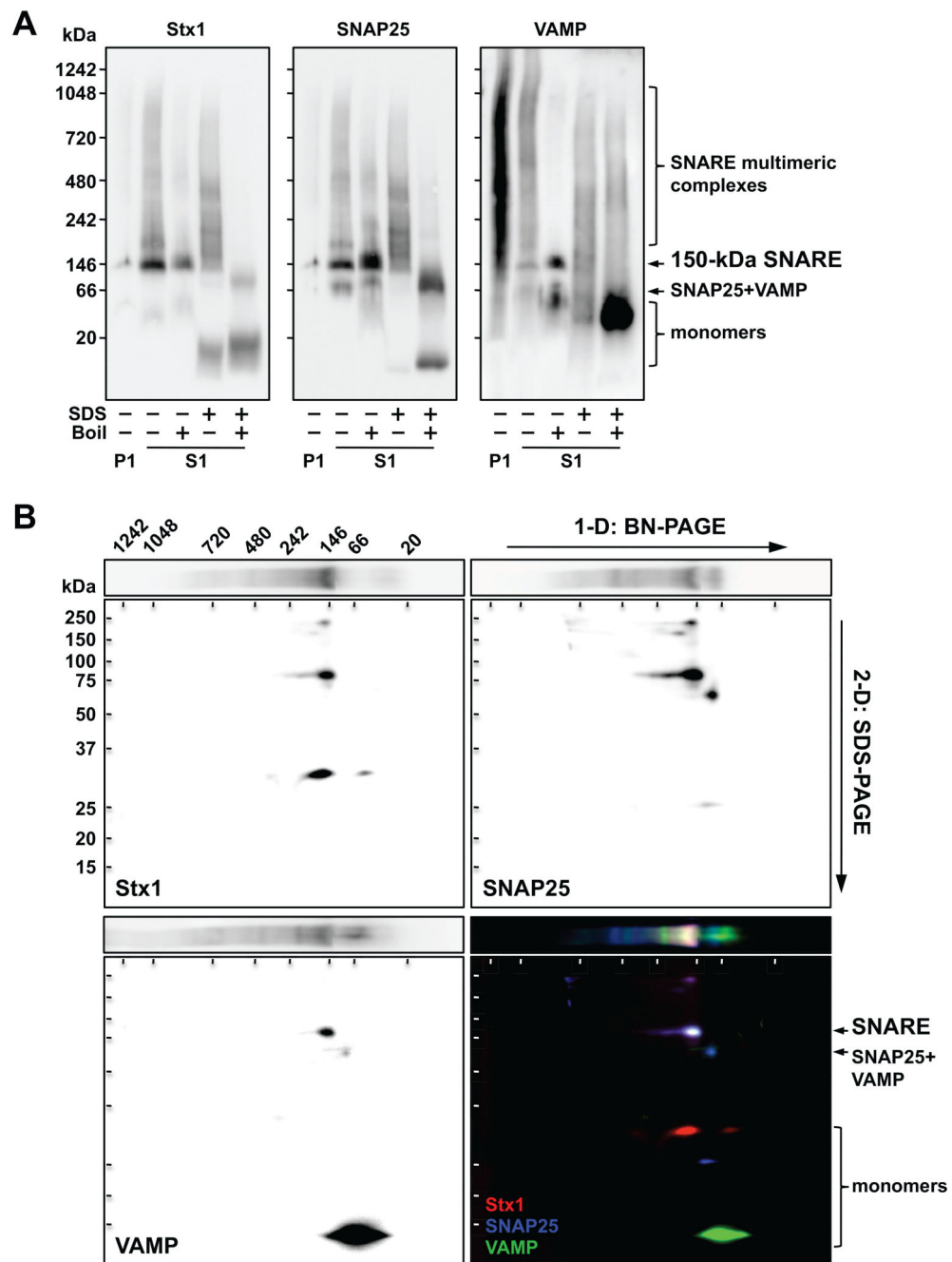


**Figure 2.** Characterization of Stx1, SNAP25 and VAMP complexes by one-dimensional (1-D) (**A**) and two-dimensional (2-D) (**B**) blue-native (BN)/SDS-PAGE. (**A**) BN gradient gels (4-16% acrylamide) were loaded with 5- $\mu$ g protein aliquots of resuspended pellets (P1) or supernatants (S1) from solubilized human cortical samples, under native conditions, or after harsh denaturation (.1% SDS and/or 5 min boiling). Protein complexes were transferred to PVDF membranes and immunoblotted with anti-Stx1 (SP7), anti-SNAP25 (SP12) or anti-VAMP (SP10) antibodies. Note that minimal SNARE protein immunoreactivity was

detected in P1 (i.e. Triton X-100-insoluble fraction) for anti-Stx1 and SNAP25 antibodies, while anti-VAMP SP10 (but not SP11) antibody detected a spurious signal (see Supplementary Figure S1C). **(B)** A BN-gel strip containing a native S1 sample in **(A)** was sliced out prior to transfer, incubated 15 min in SDS-loading buffer, and mounted onto a 12% SDS-PAGE for 2-D electrophoresis. Proteins were then transferred to PVDF membranes and sequentially probed with SP10 (green), SP7 (red) and SP12 (blue) antibodies. Captured images were arbitrarily assigned to one RGB channel and merged to visualize overlapping spots, indicating the presence of SDS-resistant complexes. **(A and B)** Molecular mass (in kDa) of native and SDS-PAGE prestained standards are shown on the left and above.

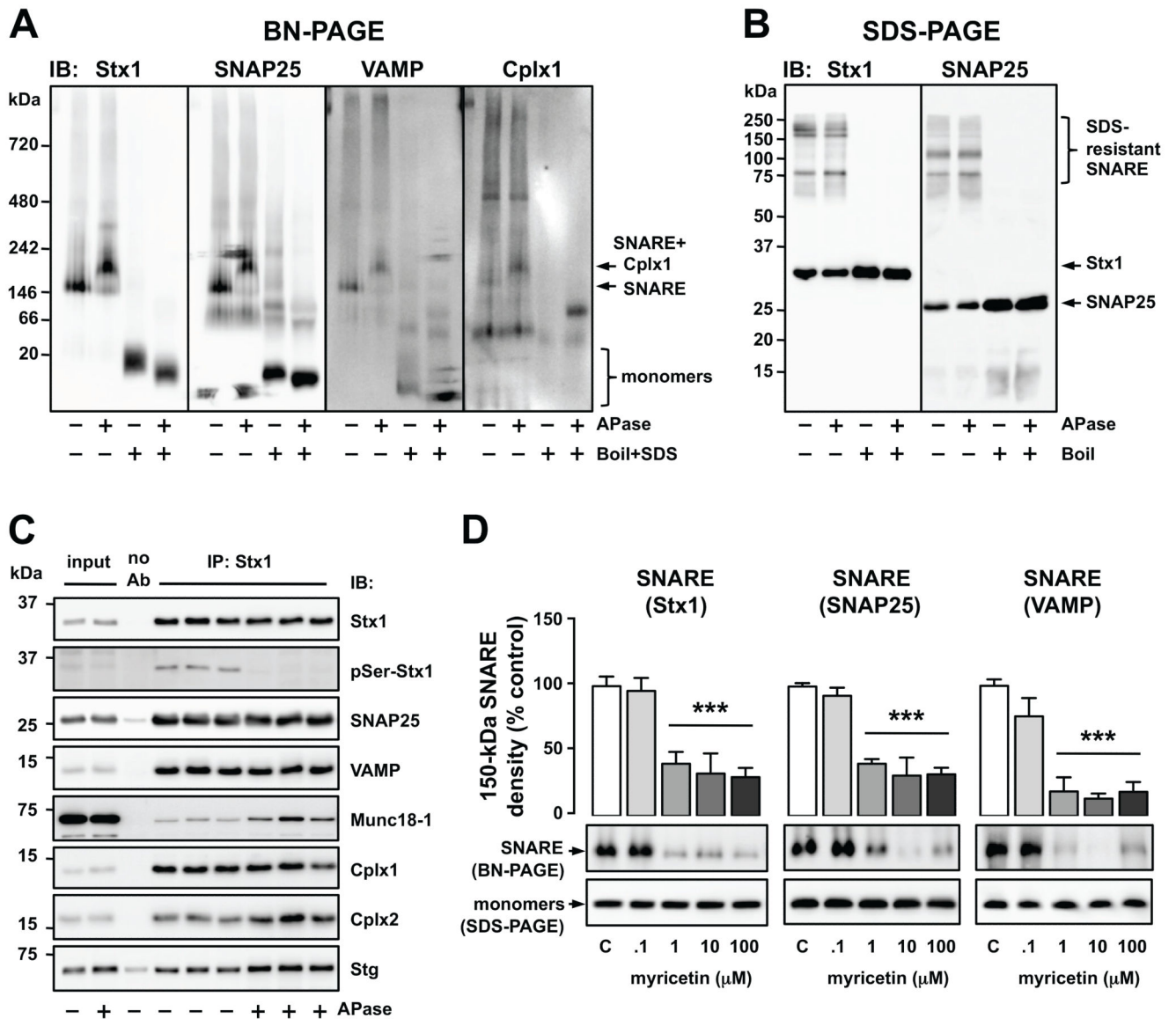


**Figure 3.**

Functional alteration of SNARE protein-protein interactions *in vitro*. (**A and B**) Solubilized protein complexes from human cortical samples were incubated in the absence or presence of alkaline phosphatase (APase; 1 U/ $\mu\text{l}$ , 1 h, 37°C) and separated by BN-PAGE (**A**) or SDS-PAGE (**B**), under native or fully denatured (.1% SDS and 5 min boiled) conditions. Proteins were transferred to PVDF membranes and immunoblotted (IB) with anti-Stx1 (SP7), anti-SNAP25 (SP12), anti-VAMP (SP11) or anti Cplx1 (SP33) antibodies. (**C**) Alternatively, triplicate aliquots of the above APase-free/treated brain homogenates were immunoprecipitated (IP) in absence (noAb) or presence of anti-Stx1 (SP7). Products were analyzed by SDS-PAGE followed by immunoblotting (IB) with target-specific antibodies. APase fully removed phosphoserine (pSer) immunoreactivity from Stx1, without altering total Stx1 signal. Student *t*-tests detected significant increases of Munc18-1 (+182%,  $p = .009$ ), Cplx2 (+68%,  $p = .002$ ), and Stg (+65%,  $p < .001$ ) in the co-IP products from APase-

treated brain homogenates compared to APase-free. **(D)** Solubilized human brain samples were incubated in the absence (controls, C) or presence of myricetin (.1-100  $\mu$ M), a functional SNARE disrupting agent. Samples were then separated by BN- or SDS-PAGE (as negative control), blotted with anti-Stx1 (SP7), anti-SNAP25 (SP12) or anti-VAMP (SP10) antibodies, and the immunodensity of the 150-kDa SNARE complex was quantified. Columns are mean  $\pm$  SEM of four replicates per experimental group of the BN-PAGE-quantified 150-kDa SNARE. One-way ANOVA detected significant differences between the groups [Stx1:  $F(4, 15) = 11.6, p < .001$ ; SNAP25:  $F(4, 15) = 20.9, p < .001$ ; VAMP:  $F(4, 15) = 19.5, p < .001$ ]; \*\*\* $p < .001$  vs control (ANOVA followed by Bonferroni's test). Representative immunoblots are shown below the plots.

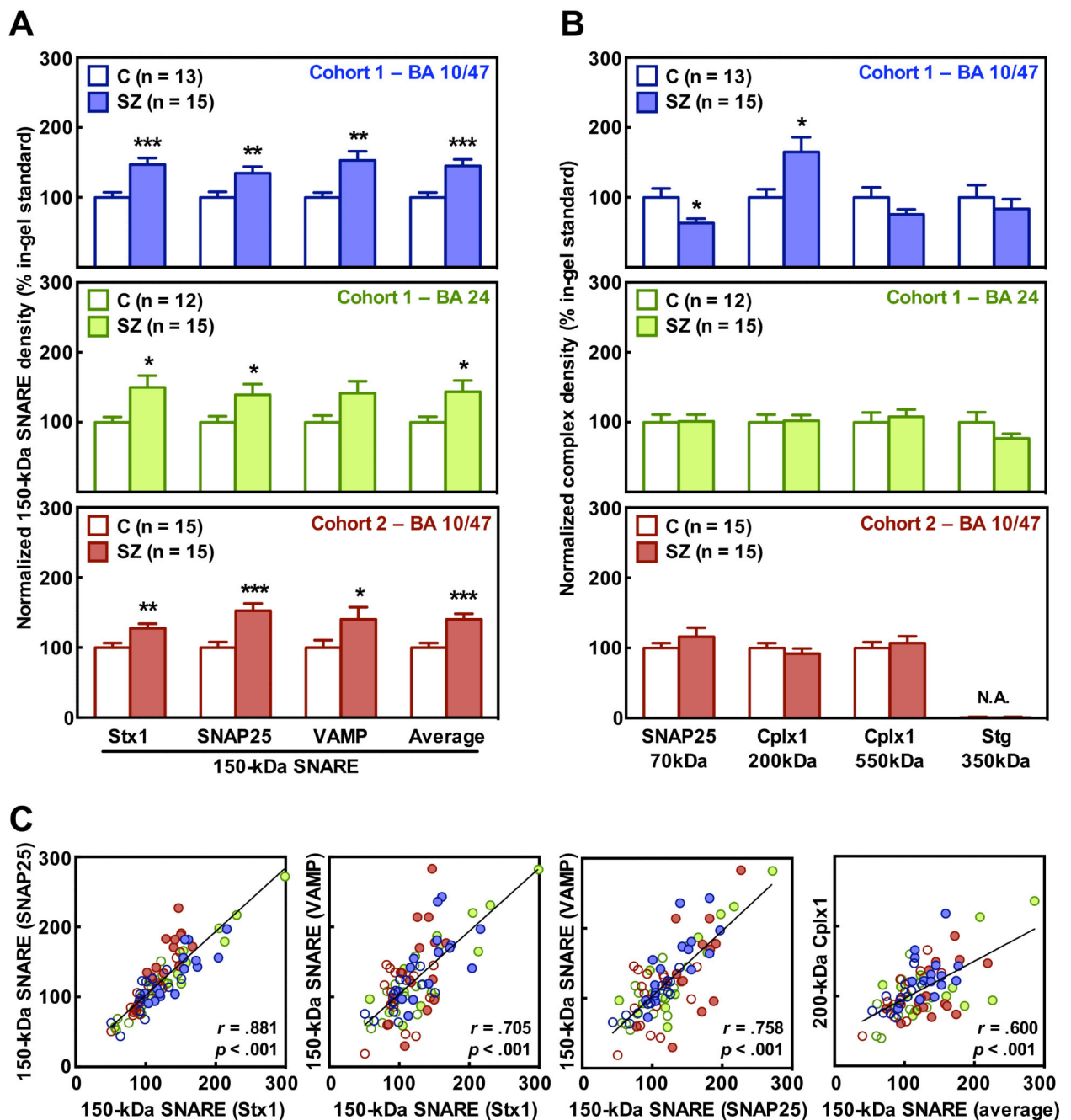


**Figure 4.**

Altered presynaptic complexes in schizophrenia orbitofrontal (OFC, BA 10/47) and anterior cingulate (ACC, BA 24) cortices. (**A and B**) Immunodensities of the 150-kDa SNARE (**A**) and other presynaptic complexes (**B**) were quantified in the OFC (blue panels) and the ACC (green panels) of schizophrenia subjects (SZ) and matched controls (C) from Cohort 1, as well as in the OFC of subjects from replication Cohort 2 (red panels), by blue native (BN)-PAGE followed by immunoblotting with anti-Stx1 (SP7), anti-SNAP25 (SP12), anti-VAMP (SP10), anti-Cplx1 (SP33), or anti-Stg (MAB48) antibodies. Values were normalized by the

total amounts of the corresponding proteins, and represented (in bars) as mean  $\pm$  SEM percentage values relative to a standard sample (pool of controls); \* $p < .05$ , \*\* $p < .01$ , \*\*\* $p < .001$  (Student's *t*-test). Quantification of the 350-kDa Stg complex was not assessed (N.A.) in the replication Cohort 2. **(C)** Scatterplots showing significant correlations between the different 150-kDa SNARE complexes measured with all three antibodies (first three panels from the left), and that of 150-kDa SNARE (average of the three measurements) and 200-kDa Cplx1 complexes (right panel), quantified in both brain regions from all subjects in Cohorts 1 and/or 2. Color patterns match those in **A** and **B**.

Author Manuscript

Author Manuscript

Author Manuscript

Author Manuscript

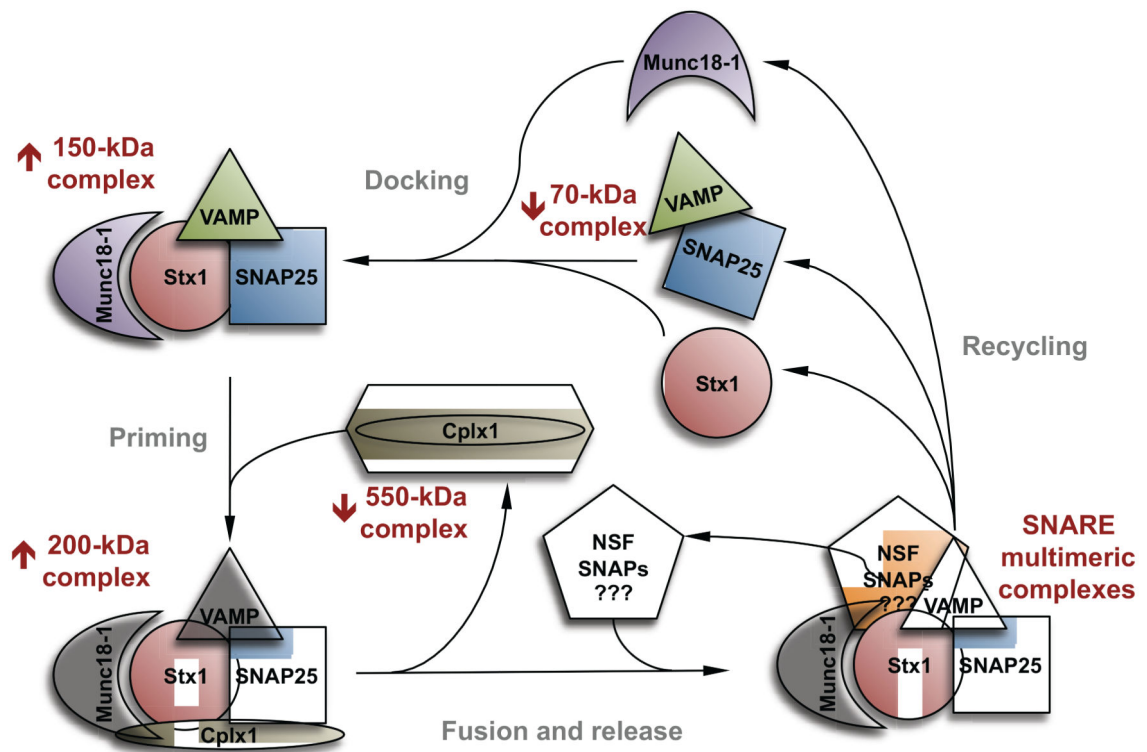


**Figure 5.**

Schematic representation of the hypothetical cycle of the presynaptic complexes involved in neurosecretion. Those complexes identified by blue native (BN)-PAGE are labeled with reddish letters, and the arrows aside indicate whether they were found upregulated (↑) or downregulated (↓) in schizophrenia orbitofrontal cortex (Cohort 1). Note that 150-kDa SNARE, and 200-kDa SNARE-Cplx1 complexes have been represented attached to Munc18-1, although no direct evidence was shown by BN-PAGE supporting the presence of this later molecule in these structures. Similarly, the presence of NSF and SNAPs in 550-kDa Cplx1 and other complexes is essentially speculative. The proposed overlapping step in the vesicle cycle is indicated with grey letters.

Table 1. Pairwise cross-correlation matrix.<sup>a</sup>

SDS-PAGE		BN-PAGE						
Sample source	Target protein	150 kDa SNARE	70 kDa SNAP25	200 kDa Cplx1	550 kDa Cplx1	350 kDa Stg		
SNAP25 co-IP products	Stx1	<i>r</i>	.4196	-.5096	-.3030	-.5613	.3745	
		<i>P</i>	.0262	.0056	.1170	.0019	.0496	
	VAMP	<i>r</i>	-.3515	.0249	-.5189	-.1445	-.1670	
		<i>P</i>	.0666	.8998	.0047	.4632	.3956	
	Munc18-1	<i>r</i>	.4028	-.3387	.5387	-.3727	-.1472	
		<i>P</i>	.0302	.0779	.0031	.0508	.4547	
	Cplx1	<i>r</i>	.5781	-.4341	.6503	-.4539	.1123	
		<i>P</i>	.0013	.0210	.0002	.0153	.5696	
	Cplx2	<i>r</i>	.1556	-.2925	.1055	-.4246	-.0887	
		<i>P</i>	.4292	.1309	.5930	.0243	.6537	
	Stg	<i>r</i>	.2750	-.2804	.2695	-.1444	.1124	
		<i>P</i>	.1567	.1484	.1655	.4636	.5690	
	Total brain homogenates	Stx1	<i>r</i>	.0456	.2931	.0553	-.0131	.0106
			<i>P</i>	.8178	.1300	.7800	.9471	.9572
SNAP25		<i>r</i>	.0756	.0873	.0047	.0953	-.0528	
		<i>P</i>	.7020	.6586	.9809	.6294	.7894	
VAMP		<i>r</i>	.0056	.3601	.0531	.3822	.1750	
		<i>P</i>	.9772	.0598	.7885	.0447	.3730	
Munc18-1		<i>r</i>	.1714	-.2161	-.0819	-.0822	-.1220	
		<i>P</i>	.3833	.2693	.6787	.6774	.5364	
Cplx1		<i>r</i>	-.0891	.1912	-.1885	.3939	-.1640	
		<i>P</i>	.6521	.3299	.3366	.0381	.4043	
Cplx2		<i>r</i>	.0452	-.1418	-.0162	.0269	-.0040	
		<i>P</i>	.8195	.4716	.9348	.8918	.9838	

<sup>a</sup>Pearson's correlation '*r*' and '*p*' values were obtained confronting data from SDS-PAGE-quantified proteins (across rows) and BN-PAGE-quantified complexes (across columns) in total homogenates and/or SNAP25 co-IP samples from the OFC (BA 10/47) of schizophrenia and control subjects in Cohort 1 (n = 28).